On the Convergence of Unsteady Generalized Aerodynamic Forces

William S Rowe*
Boeing Commercial Airplaine Company, Renton, Washington
and
Herbert J Cunningham†
NASA Langley Research Center, Hampton, Virginia

Generalized aerodynamic forces computed from analyses based on distributed pressures and finite paneling procedures are examined for solution convergence The necessity for examining the convergence of calculated forces as a function of the number of assumed pressure terms or the number of panels is well demonstrated The lifting series method converges abruptly, whereas panel methods converge gradually and monotonically for the cases analyzed An increase in wave number with increasing frequency or Mach number may cause increased computational problems coupled with increased computer usage costs With the panel methods, increase in prediction accuracy is obtained with moderate computer costs by extrapolating through the force results of two different not so fine panelings

Nomenclature

AR	= aspect ratio
ΔC_p	= lifting pressure coefficient
C	= chord length
k	= reduced frequency $\omega\ell/V$
ℓ	= reference length root half chord
M	= Mach number
N	= number of panels chordwise
s	= semispan length
q	= dynamic pressure
V	= freestream velocity (length/time)
x	= local chordwise coordinate measured from leading edge
y	= spanwise coordinate measured from midspan
ϕ_ℓ	= phase angle of lift vector
ϕ_m	= phase angle of moment vector
ω_m	= circular frequency

Introduction

NUMERICAL methods[1-5] for predicting generalized unsteady aerodynamic forces usually do not provide identical results These methods fail to agree exactly even for simple planar wing motions and results are often markedly different for control surface motions Doubts may arise concerning the validity of using any of these methods in a complex and lengthy flutter investigation Experimental methods are rarely available to verify accuracy of predicted generalized forces for complex configurations, and the flutter analyst must rely on calculated results Convergence criteria generally are not available to enable the user to obtain the best results from a particular method

Some of the problems contributing to differences in the solutions will now be identified and procedures established to ensure more consistent predictions of generalized forces A factor masking the reasons for variations in predictions is that the user works with generalized forces in performing stability analyses, and the characteristics of the pressure distributions are not visible The wavy character of the oscillatory pressure distributions is not usually displayed to alert the user to possible problems of mathematical modeling Consequently the user may not appreciate the difficulties encountered in solutions using large values of k and M where the chordwise pressures tend to become extremely wavy and more difficult to predict accurately Characteristics of chordwise pressure distributions change rapidly as the Mach number approaches 1 0 as indicated in Fig 1 The composite plot of Fig 1 represents chordwise pressure distributions calculated for several Mach numbers with $k=1\,0$ Each distribution represents chordwise pressures at the midspan station of a rectangular wing due to plunging oscillation The increase in waviness is evident even though the k value is constant

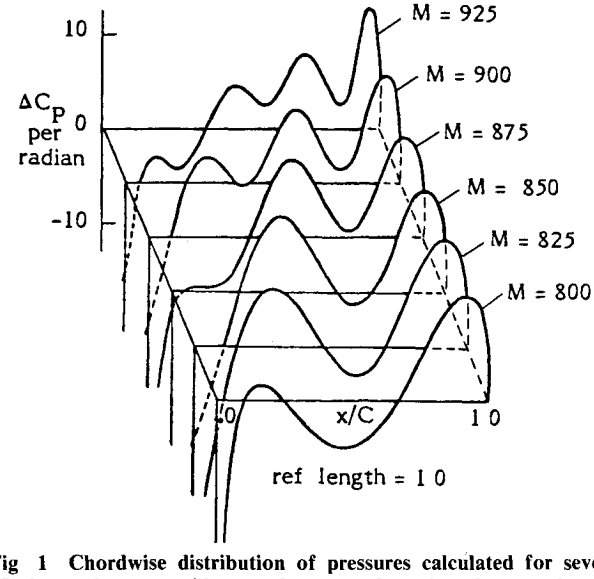

Fig 1 Chordwise distribution of pressures calculated for several Mach numbers at midspan of rectangular wing due to plunging motion at $k=1\,0$

Received March 25 1983; revision received Oct 24 1983 This paper is declared a work of the U S government and therefore is the public domain

*Senior Principal Engineer Flutter Research Group Member AIAA

†Aerospace Engineer Unsteady Aerodynamics Branch Member AIAA

Frequency of motion ω is changing in proportion to the change in Mach number (k and speed of sound are constant) Some of the waviness can be attributed to the change in frequency However, it can be shown that part of the waviness is also caused by the forward propagation of waves generated at the trailing edge The wave number (radians/reference length) associated with these forward traveling waves has been modified from that of Edwards[6] and is given as:

$$\text{Wave Number} = \frac{M}{1-M}\,\frac{k}{\ell}\,\frac{C}{2} \quad \text{(radians/semichord length)}$$

The wave number is a useful parameter for assessing the waviness of pressure distributions and estimating relative difficulties in predicting converged values of generalized forces Effects of wave number on mathematical modeling requirements are investigated in the following sections that present comparisons of generalized forces calculated for several wave number conditions Also an analysis technique is investigated for enhancing prediction accuracy of present theoretical methods with lessened computer cost

Computer Programs Used in Comparisons

Computer programs used in developing comparisons of theoretical generalized forces are:

1) RHOIV an assumed distributed pressure mode kernel function method (Refs 1 and 2)
2) SOUSSA P1 1 a velocity potential panel method (Refs 3 and 4)
3) Doublet Lattice an acceleration potential panel method (Ref 5)

RHOIV is used as a standard of reference in the following generalized force comparisons Use of RHOIV as a standard of reference must first be justified over an applicable range of wave numbers Validation is established for small wave number cases by providing comparisons of theoretical predictions and experimental data Validation is accomplished for large wave number cases (where experimental data are not available) by comparing RHOIV results with other theoretical predictions that are known to be accurate

RHOIV Validation

Small Wave Number Validation Results

RHOIV is first validated for steady flow (zero wave number) by comparison with experimental results for a tapered sweptback wing with full span trailing edge flap (Ref 7) The planform has a quarter chord sweep angle of 35 deg taper ratio of 0 5 aspect ratio of 4 5 and semispan of 0 965 m The flap chord is 27 5% of the wing chord Chordwise values of ΔC_p were measured by a single row of pressure orifices at mid semispan ($y/s = 0\ 5$) The longitudinal junction between wing and flap was sealed to prevent flow leakage between upper and lower surfaces The sealed gap satisfies the boundary conditions used in the mathematical representation of the physical model thus eliminating a common source of uncertainty in oscillatory pressure measurements involving control surfaces

Numerical investigations to determine the number of pressure terms required in kernel function analysis indicated that convergence can be achieved with six spanwise and five chordwise pressure terms It was found that boundary condition modifications of the type discussed in Ref 8 are needed to account for local variations in streamwise velocities due to thickness effects

Comparisons of theoretical and experimental results shown in Fig 2 for steady flow conditions (zero wave number) indicate that experimental results are predicted within very close tolerances even in the vicinity of the hingeline

Theoretical comparisons for another zero wave number condition but at a high subsonic Mach number are presented for the configuration shown in Fig 3 Experimental studies of this configuration were conducted as part of an investigation of active flutter suppression Experimental results are presented in Refs 9 and 10

Figure 3 also presents some convergence results for the wing with control configuration of Refs 9 and 10 These results are for $k = 0$ the zero wave number limit The convergence study was accomplished for $M = 0\ 9$ and shows wing lift due to control deflection as a function of the number of chordwise pressure terms for both nine and 13 downwash chords Clearly the lift is converged for five or more terms chordwise and the results for nine and 13 chords are virtually identical Figure 4 shows hinge moment coefficients as functions of Mach number for seven chordwise pressure terms and nine and 13 downwash chords Hinge moment coefficients (the open symbols) were obtained with no effect of airfoil thickness in RHOIV and the nine and 13 chord results are essentially identical

The solid triangles for 13 downwash chords were calculated by applying the optional provision for using the streamwise velocity component profile over the wing chord that is due solely to the airfoil thickness distributions The resulting agreement of the solid triangles and the solid curve from the experimental data of Ref 10 is very good for M up to 0 9

For small nonzero wave number RHOIV is validated against experimental results obtained by Forsching[11] for a constant chord sweptback wing with two partial span trailing edge flaps The planform has a leading edge sweep angle of 25

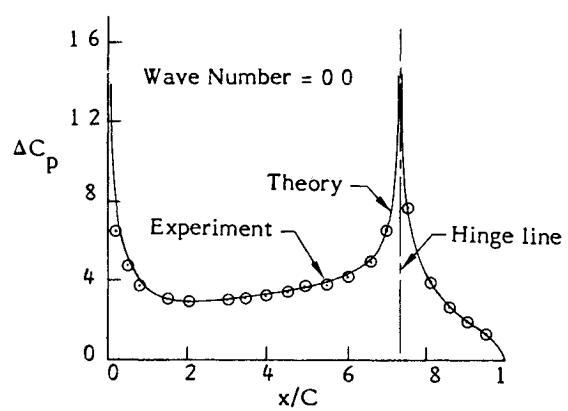

Fig 2 Theoretical and experimental pressures due to flap deflection; $\alpha = 10$ deg $M = 0\ 21$

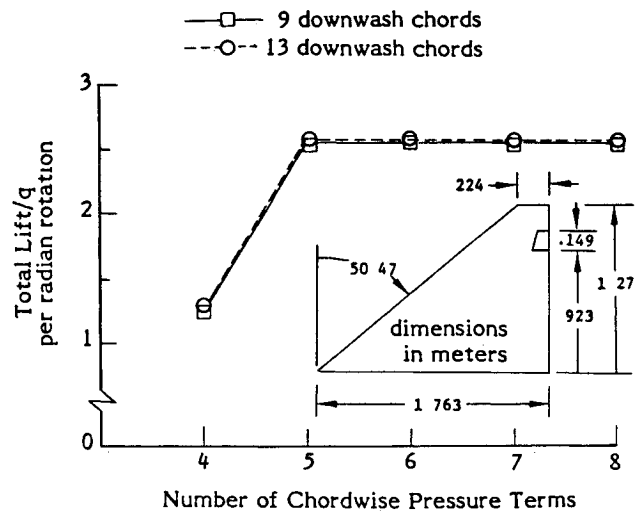

Fig 3 Convergence check of RHOIV predictions of total lift due to control surface rotation for $M = 0\ 90$ and $k = 0$

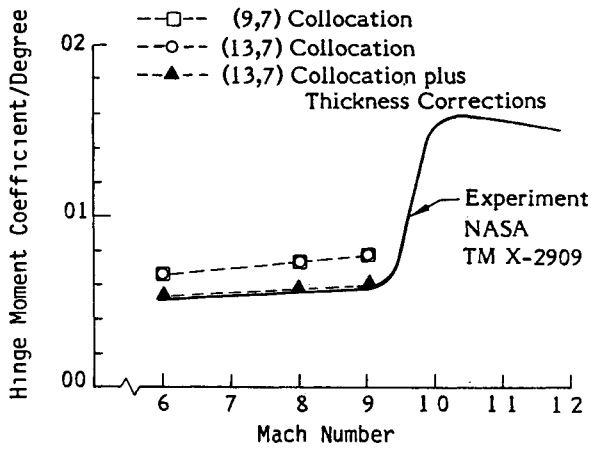

Fig 4 Experimental and theoretical steady state hinge moment coefficients for trailing edge control of NASA TM X 2909

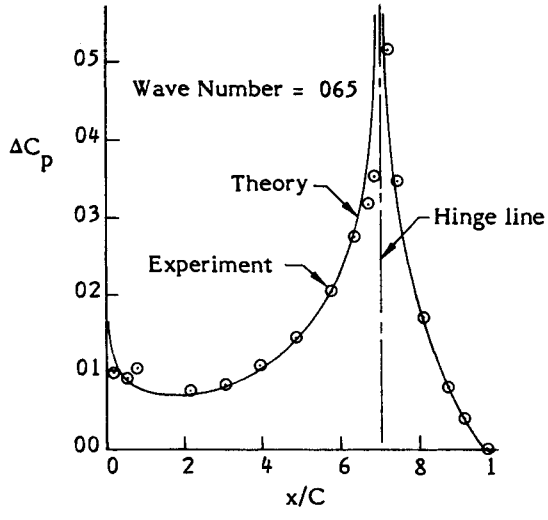

Fig 5 In phase part of chordwise pressures due to motions of outer flap; $k=0\ 372$, $M=0\ 15$

deg chord of 0 60 m and semispan of 0 88 m The flap chords are 30% of the wing chord; the inboard flap extends from $y/s=0$ to $y/s=0\ 466$ and the outboard flap from $y/s=0\ 466$ (+a gap) to $y/s=1\ 0$ Chordwise values of ΔC_p were measured by pressure orifices at five spanwise stations Gaps between the wing and the flaps were not sealed Although the configuration was tested for various combinations of wing and control surface rotations we present the results obtained for motions of the outer control surface only (inner control surface and wing maintained in a stationary position)

Preliminary convergence studies indicate that a minimum of nine spanwise and five chordwise pressure terms are required together with boundary condition modifications for thickness effects (Ref 8)

Comparisons of theoretical and experimental results shown in Fig 5 indicate that good agreement is obtained in all regions except the immediate vicinity of the hingeline where open gap boundary conditions are not accounted for in the theoretical analysis

Validation for Large Wave Numbers

Experimental data are not available for the evaluation of analytical predictions for large wave numbers Therefore in order to achieve consistency of results from different methods of analysis for large wave number conditions it is worthwhile to compare results obtained using two different prediction techniques for a common configuration

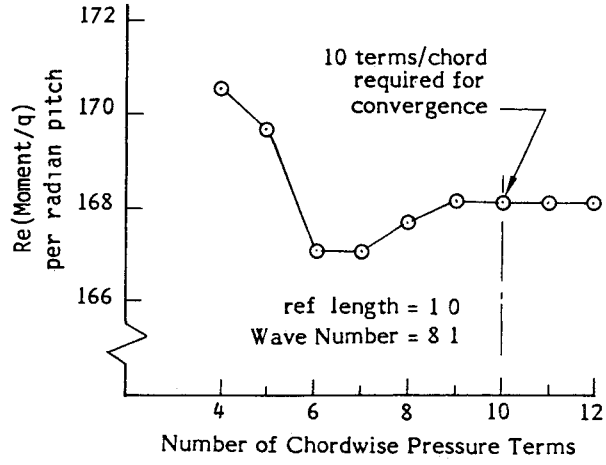

Fig 6 Convergence check of RHOIV predictions of real part of moment due to pitch on a rectangular wing of $AR=20$ for $k=0\ 9$ $M=0\ 9$

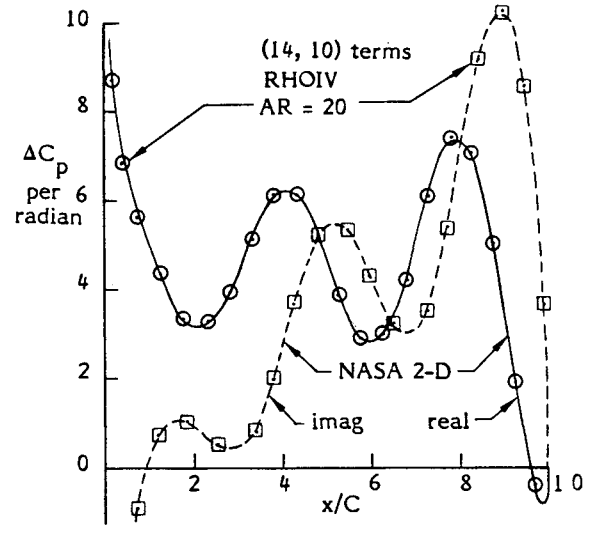

Fig 7 Comparison of thoretical predictions of pressures due to pitching about the leading edge at $k=0\ 9$ and $M=0\ 9$; wave number = 8 1

Centerline pressures for a high aspect ratio wing predicted by RHOIV are compared with two dimensional pressures from a program that is known to be accurate The two dimensional program developed at NASA Langley Research Center (LRC) (Ref 12) applies collocation procedures to solve Possio s integral equation and uses 128 collocation stations in its solution

Extremely large values of k and M not normally en countered in flutter analyses, were used to assess the accuracy of theoretical predictions for cases involving large wave numbers A study was conducted to determine the minimum aspect ratio and minimum number of assumed pressure modes necessary to approximate two dimensional flow conditions closely at the centerline of a rectangular wing that is pitching about the leading edge at $M=0\ 9$ and $k=0\ 9$ For a given aspect ratio (Fig 6) the minimum number of spanwise and chordwise pressure terms are determined to achieve convergence for that particular aspect ratio Converged centerline pressures are then compared to two dimensional pressures (from NASA LRC) to determine whether the aspect ratio is large enough to provide two dimensional charac teristics at the centerline of the planform

If the predicted pressures fail to correlate closely with the two dimensional pressures the study is repeated for a larger aspect ratio

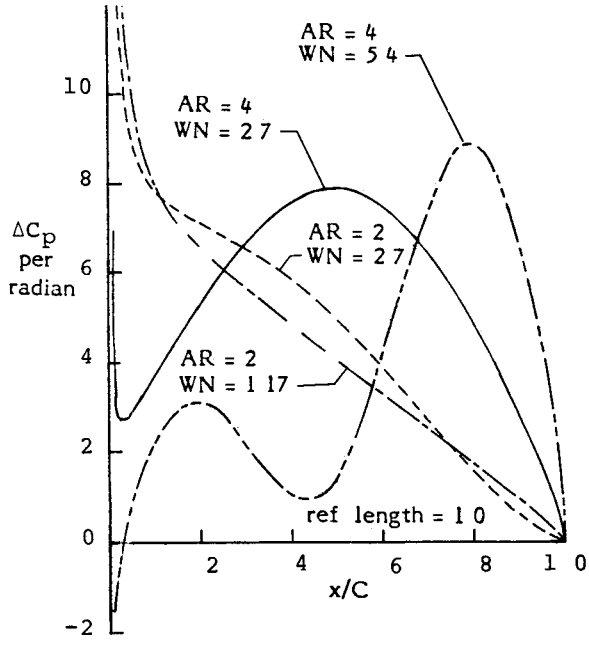

Fig 8 Real part of midspan pressures on rectangular planforms caused by pitching about the trailing edge for several wave numbers

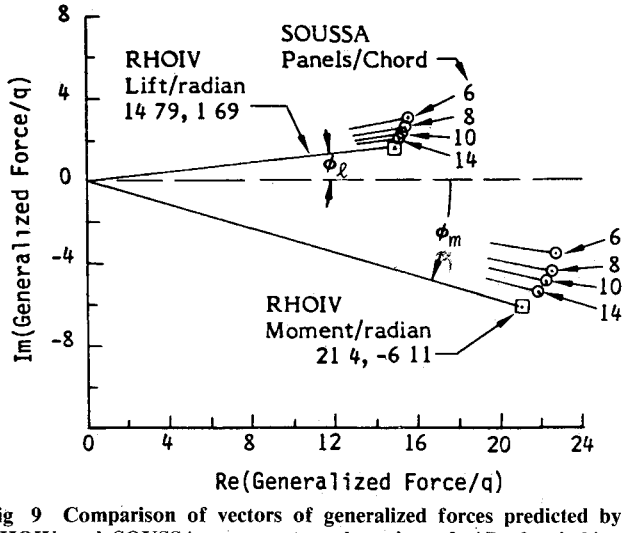

Fig 9 Comparison of vectors of generalized forces predicted by RHOIV and SOUSSA on a rectangular wing of $AR=2$ pitching about the trailing edge at $k=0\ 5$, $M=0\ 7$, wave number = 1 17

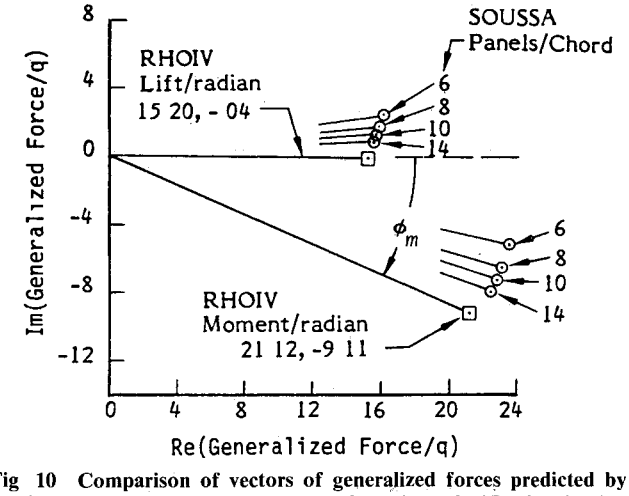

Fig 10 Comparison of vectors of generalized forces predicted by RHOIV and SOUSSA on a rectangular wing of $AR=2$, pitching about the trailing edge at $k=0\ 3$ $M=0\ 9$ wave number = 2 7

Table 1 Chordwise pressure terms required for convergence for lift and moment calculations (pressure terms/chord)

AR	k	M	WN	Lift	Moment
2	0 5	0 7	1 17	3	4
2	0 3	0 9	2 7	4	5
4	0 3	0 9	2 7	6	7
4	0 6	0 9	5 4	8	9

Results of the study indicate that two dimensional flows are developed at the centerline of a rectangular wing of $AR \geq 20$ Accurate predictions require 14 spanwise and 10 chordwise pressure terms in the three dimensional simulation of two dimensional flows as indicated by Figs 6 and 7

The foregoing has demonstrated that RHOIV does provide accurate predictions of generalized forces over a large range of wave numbers Consequently RHOIV will be used as a standard of reference in the following comparisons of generalized forces calculated by two distinctly different panel methods

Generalized Forces of Panel Methods

Generalized force calculations are presented for several wave number cases to assess convergence characteristics of finite panel methods For brevity only the final converged RHOIV results will be presented in the comparisons

Planar Lifting Surface Comparisons

Generalized force calculations are given for two simple rectangular planforms and a rectangular wing control surface configuration

The analysis parameters for the cases investigated are:

(1) $AR=2$ $k=0\ 5$ $M=0\ 7$ (wave number = 1 17)

(2) $AR=2$ $k=0\ 3$ $M=0\ 9$ (wave number = 2 7)

(3) $AR=4$, $k=0\ 3$ $M=0\ 9$ (wave number = 2 7)

(4) $AR=4$ $k=0\ 6$ $M=0\ 9$ (wave number = 5 4)

Figure 8 represents converged chordwise pressures of RHOIV that are calculated for the midspan station of the rectangular planforms that are oscillating in pitch about the trailing edge for the reduced frequencies and Mach numbers defined above The term Wave Number is abbreviated as WN in Fig 8

The pressures become more oscillatory with increasing wave number and it is self evident that the number of chordwise terms must be increased for increasing wave number in order to satisfy accuracy requirements

A summary of the number of chordwise pressure terms required for convergence for lift and moment calculations is given in Table 1

Theoretical comparisons between the converged RHOIV solutions and the two previously mentioned panel methods are now presented for the above analysis cases

The first comparison developed is for a rectangular wing of $AR=2$ that is pitching about the trailing edge at $M=0\ 7$ and $k=0\ 5$ Generalized force vectors obtained from SOUSSA P1 1 are shown in Fig 9 for several paneling arrangements Each paneling arrangement provided equal numbers of spanwise and chordwise subdivisions Spanwise panel lengths vary according to a cosine distribution; chordwise lengths are equal

SOUSSA predictions appear to be approaching con vergence with increasing density of chordwise panels with lift predictions tending to be more accurate than moment predictions

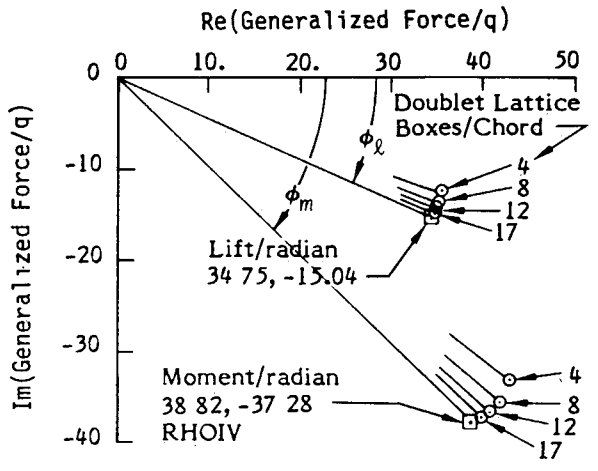

Fig 11 Comparison of generalized force vectors predicted by RHOIV and Doublet Lattice on a rectangular wing of $AR=4$, pitching about the trailing edge at $k=0\,3$ $M=0\,9$, wave number $=2\,7$

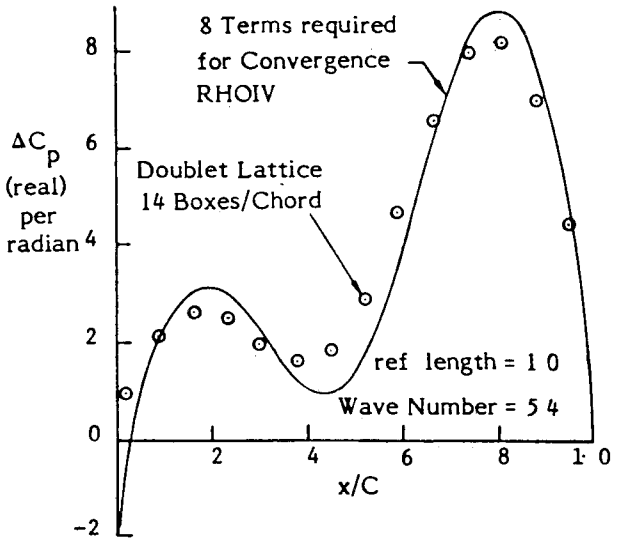

Fig 13 Real part of pressures near midspan of an $AR=4$ wing for $k=0\,6$ and $M=0\,9$

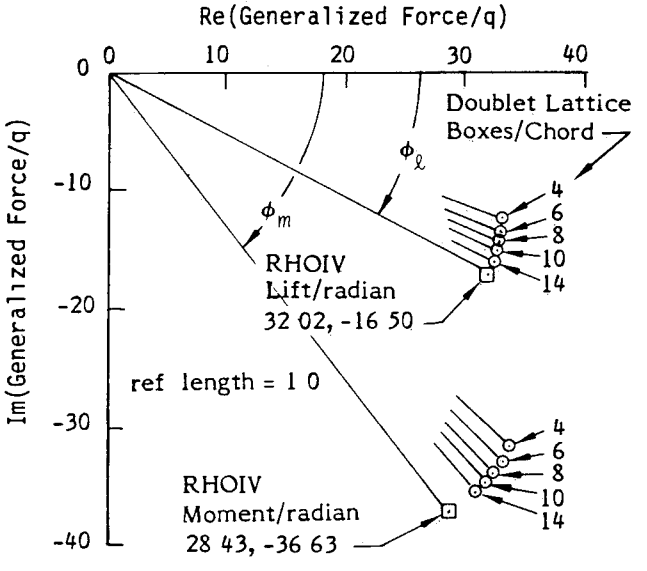

Fig 12 Comparison of generalized force vectors predicted by RHOIV and Doublet Lattice on a rectangular wing of $AR=4$ pitching about the trailing edge at $k=0\,6$ $M=0\,9$ wave number $=5\,4$

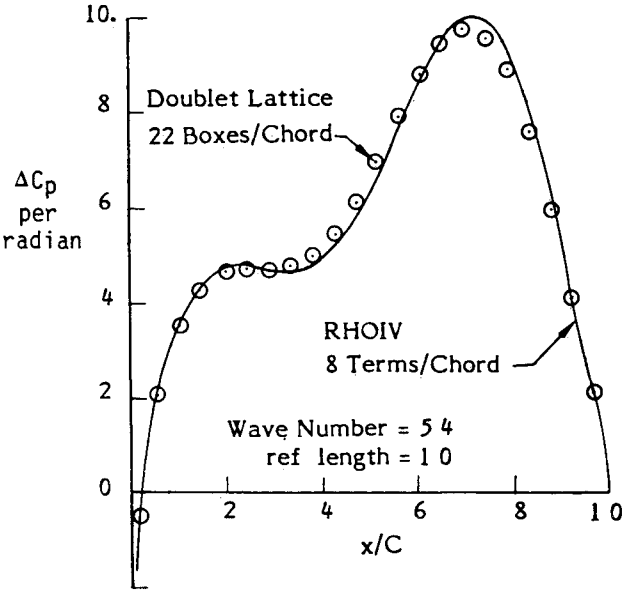

Fig 14 Real part of pressures near midspan of an $AR=2$ wing for $k=0\,6$ and $M=0\,9$

In the next case the aspect ratio is maintained at $AR=2$ but a change in wave number (from 1 17 to 2 7) causes a distinct bulge in the pressures to appear in the midchord region (Fig 8) This change in the pressure distribution requires an increase in the number of chordwise panels in order to maintain the same accuracy

Generalized force vectors from SOUSSA for this case shown in Fig 10 are further displaced from the converged values than noted for the previous case That is the phase error for the 14 panel arrangement is about the same as the phase error of the ten panel arrangement of the previous comparison

The next comparison involves only a change in planform aspect ratio while maintaining the wave number at 2 7 Centerline pressures obtained for an $AR=4$ planform (Fig 8) are dramatically different than those predicted for the wing of $AR=2$ Increased complexity of the pressure distribution in the midchord region requires even more RHOIV assumed pressure modes to satisfy convergence This illustrates the point that convergence is dependent upon planform shape as well as the value of the wave number

Figure 11 shows generalized force vectors predicted by Doublet Lattice for the $AR=4$ planform and a wave number $=2\,7$ In Doublet Lattice paneling all panels were required to be of equal size (in any one arrangement) with local panel aspect ratio never exceeding a value of 1 5 Comparison of Fig 11 with Fig 10 indicates that convergence appears to be faster for the Doublet Lattice method than for SOUSSA

The final comparison for simple planforms is presented to evaluate convergence for $k=0\,6$ the highest k value that can be used with confidence in linearized theoretical predictions (Ref 13)

Generalized force vectors shown in Fig 12 for a rectangular wing of $AR=4$ and wave number $=5\,4$ appear to be converging with increasing density of chordwise panels However convergence is proceeding at an ever diminishing rate A maximum of 14 panels per chord was used in the

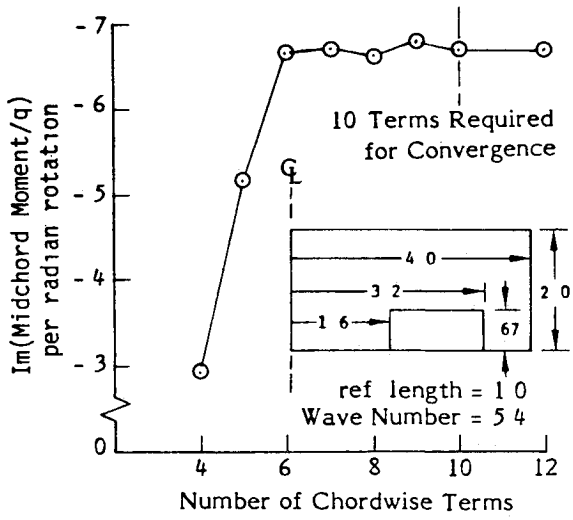

Fig 15 Convergence plot of out of phase part of moment about midchord due to control surface motions for $k=0\ 6$, $M=0\ 9$

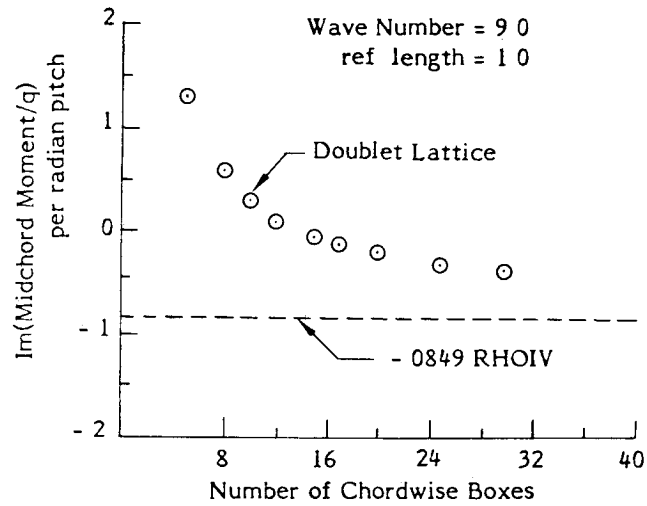

Fig 17 Doublet Lattice predictions of midchord moment as function of the number of chordwise boxes for a rectangular wing of $AR=2$ with $k=1\ 0$, $M=0\ 9$

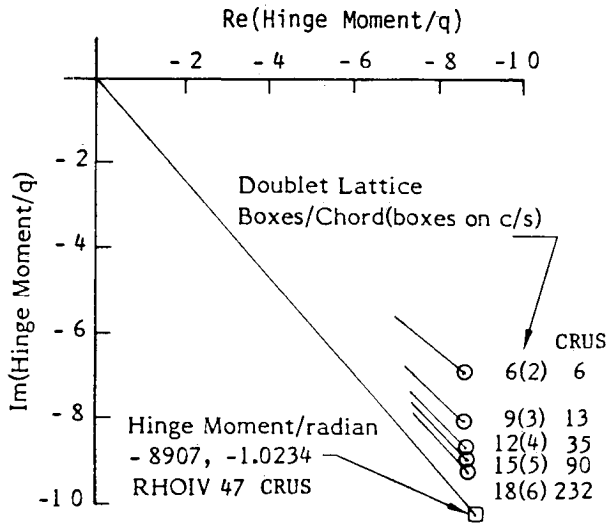

Fig. 16 Hinge moment vectors due to control surface motions for a wave number of 5 4

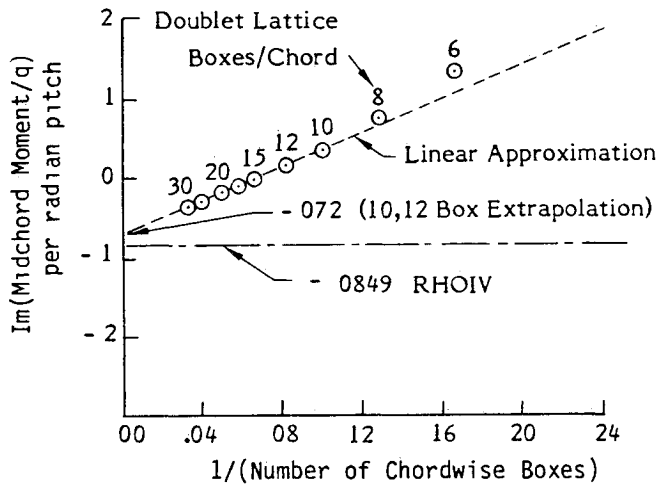

Fig 18 Imaginary part of moment due to pitching about the mid chord of a rectangular wing of $AR=2$ for $k=1\ 0$, $M=0\ 9$, plotted against the inverse of the number of chordwise boxes

analysis because of program limitations on the total number of panels that may be distributed over the lifting surface

A comparison of pressures calculated by RHOIV and Doublet Lattice for this case is shown in Fig 13 The Doublet Lattice pressure distribution for 14 boxes/chord does appear to be approaching convergence However the comparison does not establish whether the Doublet Lattice pressures are approaching the converged RHOIV solution or are con verging to some other distribution

It is evident that in order to evaluate the convergence process the chordwise panel density must be increased For this purpose the aspect ratio is changed from $AR=4$ to $AR=2$ to reduce the number of spanwise panels for an in crease in chordwise density while maintaining the same program limit for total number of panels

The pressure comparison of Fig 14 indicates that the Doublet Lattice predictions are approaching the same limit given by RHOIV It is speculated that almost identical results could be achieved if the Doublet Lattice paneling density were increased even further

Hinge Moment Comparisons

Hinge moment comparisons are provided for the con figuration sketched on Fig 15 for $k=0\ 6$ and $M=0\ 9$ The selected k value represents the largest usable value compatible with linearized assumptions (Ref 13) Results of RHOIV convergence studies shown in Fig 15 indicate that ten chordwise pressure terms are sufficient to satisfy accuracy requirements

Comparison of hinge moment vectors are shown in Fig 16 for several Doublet Lattice paneling arrangements The first number associated with Doublet Lattice solutions represents the total number of panels on each chordwise segment The second bracketed number is the number of chordwise panels on the control surface The third number represents the total computer usage costs given by the acronym CRUS

Results of the above comparisons indicate that finite paneling methods will provide the same prediction accuracy as the distributed pressure kernel function approach provided the number of chordwise panels is allowed to increase suf ficiently However due to budget constraints and program limitations this may never be achieved by present procedures Thus we seek to define extrapolation procedures to estimate converged values for reasonable computer usage costs

Extrapolation-to-Convergence

Figure 17 shows a comparison of predictions for the aerodynamic moment developed on a rectangular wing of

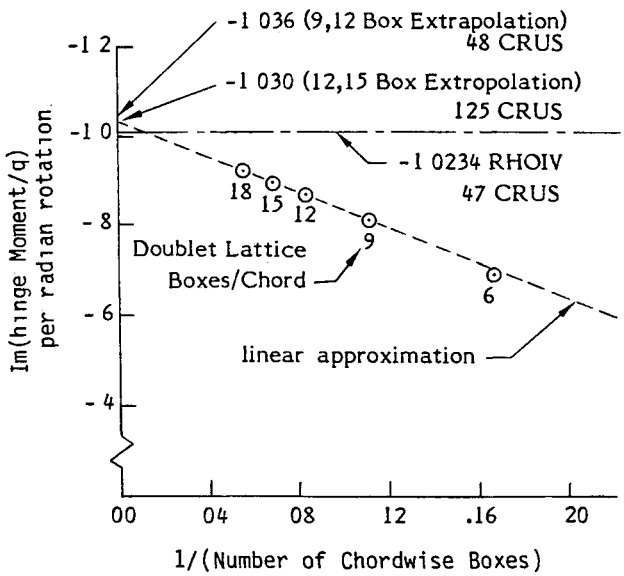

Fig 19 Extrapolation of Doublet Lattice predictions of the imaginary part of hinge moments of Fig 16

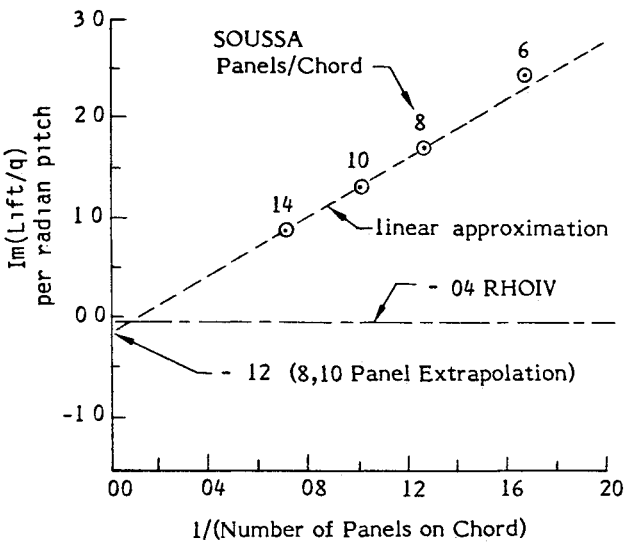

Fig 20 Extrapolation of SOUSSA predictions of the imaginary part of lift of Fig 10

$AR=2$ that is pitching about its midchord at $M=0\,9$ for an extreme value of reduced frequency $k=1\,0$ The Doublet Lattice predictions appear to be approaching convergence but at an ever diminishing rate Consideration of the locus of Doublet Lattice predictions shows that the radius of curvature appears to be approaching ∞ for very large values of N This suggests that a linear representation would suffice for large N if the abscissa were changed to $1/N$

Such is the case as in Fig 18 where it is shown that the generalized forces lie almost on a straight line for $N\geq 10$ Adjacent line segments through the data points have slightly different slopes but these differences in slopes rapidly ap proach zero as N becomes large Using a straight line ex trapolation through points for $N=10$ and 12 produces a pitch moment value of $-0\,072$ which compares favorably with the result of RHOIV

An extrapolation of hinge moment values of Fig 16 is shown in Fig 19 Straight line extrapolation of predictions based on $N=9$ and 12 provides a result that closely ap proximates the converged RHOIV result Total computer usage costs incurred for the two analyses is 48 CRUS which is almost identical to that of RHOIV 47 CRUS

Extrapolation of Fig 10 SOUSSA predictions shown in Fig 20 indicate that more accurate predictions are also at tainable by extrapolation for this paneling method.

Conclusions

Comparisons of predicted generalized forces indicate that convergence becomes increasingly difficult to attain with increasing wave number Generalized forces predicted by three theoretical methods are essentially equivalent, provided that sufficient density in chordwise paneling is provided in the paneling arrangements

It is suggested that a preliminary convergence study be performed prior to any extensive flutter analysis by calculating generalized forces for the most complicated camber bending mode shape and using the largest analysis wave number The generalized forces should be plotted against the number of assumed pressure modes for the distributed pressure kernel function method, to determine requirements for convergence Converged generalized forces for subsequent flutter analyses are then obtained for all lesser wave numbers by using the minimum number of pressure terms that satisfy convergence requirements for the largest wave number and most complicated mode shape For the paneling methods the generalized forces are calculated for different panel densities and plotted against $1/N$ (inverse of number of chordwise panels) Paneling arrangements should provide a number of chordwise panels sufficient to ensure that predicted generalized forces will be contained in the region where linear variation with $1/N$ is attained Accuracy and cost estimations are made for extrapolating forces to $1/N\rightarrow 0$ to provide a basis for selecting the most appropriate combination Once two paneling arrangements have been selected generalized forces are calculated for each arrangement (for all lesser wave numbers) and extrapolation procedures applied to attain convergence for each member of the generalized force matrix used in the flutter analysis

References

[1] Rowe W S Sebastian J D and Petrarca J R Reduction of Computer Usage Costs in Predicting Unsteady Aerodynamic Loadings Caused by Control Surface Motions Analysis and Results ' NASA CR 3009 March 1979

[2] Petrarca J R , Harrison B A Redman M C , and Rowe W S Reduction of Computer Usage Costs in Predicting Unsteady Aerodynamic Loadings Caused by Control Surface Motions—Computer Program Description NASA CR 145354 June 1978

[3] Morino L Steady Oscillatory and Unsteady Subsonic and Supersonic Aerodynamics —Production Version 1 1 (SOUSSA P1 1) Vol I Theoretical Manual NASA CR 159130 Jan 1980

[4] Morino L , Steady Oscillatory and Unsteady Subsonic and Supersonic Aerodynamics —Production Version 1 1 (SOUSSA P1.1) Vol II User/Programmer Manual NASA CR 159131 Jan 1980

[5] Giesing, J P Kalman T P and Rodden W P Subsonic Unsteady Aerodynamics for General Configurations, Part I Vol 1: Direct Application of the Non Planar Doublet Lattice Method AFFDL TR 71 5 Part I Feb 1971

[6] Edwards, J W Applicatins of Laplace Transform Methods to Airfoil Motion and Stability Calculations AIAA/ ASME/ASCE/AHS 20th Structures, Structural Dynamics and Materials Conference St Louis Mo April 4 6 1979

[7] Tinling B E and Dickson J K Tests of a Model Horizontal Tail of Aspect Ratio 4 5 in the AMES 12 Foot Pressure Wind Tun nel NACA RM A9G13 1949

[8]Rowe W S Redman M C Ehlers F E and Sebastian J D Prediction of Unsteady Aerodynamic Loadings Caused by Leading Edge and Trailing Edge Control Surface Motions in Subsonic Compressible Flow—Analysis and Results NASA CR 2543 May 1975

[9]Abel I and Sandford M C , Status of Two Studies on Active Control of Aeroelastic Response ' NASA TM X 2909 Sept 1973

[10]Rainey A G Ruhlin C L and Sandford M C Active Control of Aeroelastic Response AGARD CR 119 pp 16 1 to 16 8

[11]Forsching H Triebstein H and Wagener J AGARD CP 80 70 Symposium on Unsteady Aerodynamics for Aroelastic Analysis of Interfering Surfaces Part II pp 15 1 to 15 12

[12]Bland S R Development of Low Frequency Kernel Function Aerodynamics for Comparison with Time Dependent Finite Dif ference Methods NASA Technical Memorandum 83283 May 1982

[13]Satyanarayana, B and Davis S Experimental Studies of Unsteady Trailing Edge Conditions *AIAA Journal* Vol 16 Feb 1978